



**Insights into Phases of Liquid Water from Study of
Its Unusual Glass-Forming Properties**

C. Austen Angell, *et al.*

Science **319**, 582 (2008);

DOI: 10.1126/science.1131939

***The following resources related to this article are available online at
www.sciencemag.org (this information is current as of February 1, 2008):***

Updated information and services, including high-resolution figures, can be found in the online version of this article at:

<http://www.sciencemag.org/cgi/content/full/319/5863/582>

This article **cites 88 articles**, 8 of which can be accessed for free:

<http://www.sciencemag.org/cgi/content/full/319/5863/582#otherarticles>

This article appears in the following **subject collections**:

Chemistry

<http://www.sciencemag.org/cgi/collection/chemistry>

Information about obtaining **reprints** of this article or about obtaining **permission to reproduce this article** in whole or in part can be found at:

<http://www.sciencemag.org/about/permissions.dtl>

Insights into Phases of Liquid Water from Study of Its Unusual Glass-Forming Properties

C. Austen Angell

The vitrification of pure water is compared with that of molecular solutions rich in water, and gross differences are noted. Thermodynamic reasoning and direct observations on noncrystallizing nanoconfined water indicate that the glass transition in ambient-pressure water is qualitatively distinct from that found in the usual molecular liquids. It belongs instead to the order-disorder class of transition seen in molecular and ionic crystalline materials. The distinctive “folding funnel” energy landscape for this type of system explains the extreme weakness of the glass transition of water as well as the consequent confusion that has characterized its scientific history; it also explains the very small excess entropy at the glass transition temperature. The relation of confined water behavior to that of bulk is discussed, and the “fragile-to-strong” transition for supercooled water is interpreted by adding a “critical point-free” scenario to the two competing scenarios for understanding supercooled bulk water.

Many aspects of water’s liquid-state behavior are unusual, and this includes the way in which it forms a glass. For most molecular liquids, particularly in small samples, rapid cooling generates a glassy solid rather than a crystalline phase. Vitrification in most cases has a clear thermodynamic signature—a rapid drop in heat capacity—as the translational and reorientational degrees of freedom, by which the liquid absorbs energy and flows, are frozen out. Water is exceptional in this regard in that its glass formation signature is very weak, so much so that the glass transition temperature T_g , typically assigned in the range from 120 to 160 K, has been controversial. In this review I argue that the various experimental and theoretical arguments about the glass transition in water can be reconciled in terms of an order-disorder transition that occurs in the “anomalous regime,” 150 to 250 K (1–3). This order-disorder transition, which may include some weak first-order character, effectively steals the disordering heat capacity of the normal glass transition, leaving almost nothing to observe at the temperature predicted by T_g extrapolations from binary-solution glasses.

What Is the Glass Transition?

The glass transition is not a “transition” in the thermodynamic sense of the word (4). With the glass transition, everything depends on time, and so T_g can only be given a firm value when the time rate of change of temperature (heating or cooling) has been fixed. Then it is straightforward to say what the glass transition is, in terms of some basic property such as heat capacity. The glass transition is that phenomenon in which the heat capacity increases abruptly during heating,

as previously frozen degrees of freedom are excited. The heat capacity changes from a value characteristic of a solid (only vibrational degrees of freedom, often the Dulong and Pettit value) to the higher value characteristic of a liquid—and there is usually a big difference, making it easy to detect. For instance, in a glass-forming solution containing two parts of water and one part of its look-alike, hydrogen peroxide (H_2O_2 , melting point $T_m = 271.5$ K), the heat capacity more than doubles at the glass transition (5). The same is found when the solution contains, in place of H_2O_2 , the other water look-alike, hydrazine [N_2H_4 , $T_m = 5.5^\circ\text{C}$ (5)] (Fig. 1).

The glass transition also has flow consequences. Above its T_g , the substance, when stressed, flows like a liquid—but it flows very slowly, unless $T \gg T_g$. Below T_g (6–8), it bends elastically like a solid, and then splinters—unless time is first allowed to pass, when again it flows (8). Why? Well, the extra time that passed was equivalent to a lowering of the T_g . The glass transition occurs when (9) the condition

$$d\tau/dT \cdot dT/dt (= Q \cdot dT/dt) \approx 1 \quad (1)$$

is met, where Q is the cooling rate, t is time, and τ is the “relaxation time”.

In some liquids, those in the “fragile” class (10), the change in heat capacity at T_g happens very sharply and is complete in just a few degrees, because a fragile liquid is one whose relaxation time changes very rapidly, in “super-Arrhenius” fashion, with temperature. In non-fragile liquids, however, it may take tens of degrees, even hundreds in the case of “strong” liquids with high T_g values [this is also true for ordinary liquids studied on computer simulation time scales, e.g., 50°C for SPC-E water (11)]. The hydrazine solution in Fig. 1, for instance,

although having a very large heat capacity change, is not a fragile liquid (12). It requires some 20 K to complete its transition. It is a part of the controversy concerning water that some authors consider it to be a strong liquid near its T_g (13–17), whereas others have argued that it is very fragile (18, 19) and still others think it is both (14), depending on the temperature and the cooling rate.

The Problem with Water and Its T_g

The large change in heat capacity ΔC_p at T_g for $(\text{H}_2\text{O})_2 \cdot \text{H}_2\text{O}_2$ (and the comparably large ΔC_p for $\text{H}_2\text{O} \cdot \text{N}_2\text{H}_4$) renders the T_g determinations in these cases quite unambiguous. However, in the phenomenon usually considered to be the glass transition of laboratory water (Fig. 1), the value of ΔC_p is tiny, only 2% of that for the above aqueous solutions (20, 21). When a glass transition is so feeble, it is quite difficult to detect. Experienced glass researchers have missed it completely (22, 23). Yue and the author (24) suggested such a weak effect might be rationalized as an “annealing pre-peak,” the real T_g being inaccessible because of crystallization, but there are alternatives to consider. What other reason could there be for the difference between water and its solutions? We provide an answer below.

Note that the glassy water for which the above small value of ΔC_p was recorded was made from the liquid state by hyperquenching (25) and is called hyperquenched glassy (HQG) water. Other ways of making glassy water exist, some of them exotic (3). The most common method and the earliest reported (26)—and also the way glassy water forms in nature—is by vapor deposition on a cold surface. [Condensed on cosmic dust particles and agglomerated into comets, this form, called low-density amorphous (LDA) water, is believed to be the most abundant form of water in the universe.] Another method, more recent and quite exotic, is by compression of ordinary ice (I_h) until amorphized (27), followed by decompression with annealing. The latter process converts the initial high-density amorphization product HDA into LDA. The three forms, HQG and the two LDAs, are almost identical in structure, although the form obtained by the high-pressure route shows some differences in thermal behavior that are not removed by heating above 136 K, when structural differences between glasses of the same glass prepared by different routes would be expected to disappear (28). Each of these preparations manifests comparably feeble heat capacity jumps at the annealing-induced thermal event, usually close to 136 K (29, 30). But in the HDA \rightarrow LDA case (29), a heat capacity scan, made at a rate slower by a factor of 120 than the others, found T_g at 124 K (without annealing), which is 12 K below the usual value and 17 K below the “annealing-free” (20 K/min) scan value, 141 K, reported in (20) and (24).

An important part of the problem in characterizing water through its glass transition is that

Department of Chemistry and Biochemistry, Arizona State University, Tempe, AZ 85287, USA. E-mail: caa@asu.edu

water is a very bad glass-former. This means that the glassy state does not survive heating much above the putative T_g of 136 K. Indeed, in Handa and Klug's low-scan rate study (29) it crystallized at 132 K. In a "standard" scan [20 K/min, see (6)], LDA crystallizes in the range 150 to 160 K, depending on the manner of preparation. Thus, there is a gap [or a "no-man's land" (31)] between 150 and 236 K (the limit of supercooling) in which no direct data are available for bulk, or even microscopic ($\sim 1 \mu\text{m}$), water (although there are insights from nanoconfined water; see below).

In Fig. 1, what has been reviewed up to this point is summarized as the heat capacity changes at T_g for water and its solutions as well as for the higher-temperature liquid states of water and its solutions, both molecular and ionic. The behavior of water in the region immediately below its freezing point (5, 32, 33) is especially noteworthy. Although criticized as artifactual (34), it has recently been established as correct by bulk water (10-ml samples of extreme purity) studied to -30°C (35). The hydrazine solution data in Fig. 1 may be interpreted as how water would behave if it could not form an open tetrahedral network through hydrogen bonding.

The challenge brought into focus by Fig. 1 is to find out what happens in the "gap" for the case

Although the possibility of a weak first-order phase transition en route is not excluded (see below), we look for the behavior along a continuous path in C_p between the large and anomalously increasing value around 240 K, and the tiny value at 150 K.

Insights from Nanoscopic Water

The problem of how water should behave if crystallization did not occur was addressed some time ago by applying thermodynamic principles to data available from both below and above the gap (15). The results will be revisited below, but there is also a more direct route: by studying water in nanoscopic confinement. Water near surfaces often does not crystallize upon cooling, but only recently have the properties of such water been measured. The heat capacity of nanoscopically confined water was reported by the Oguni group (38, 39), who used measurements on water in nanoporous media of different pore sizes to separate the properties of "surface water" from those of "internal" water in their noncrystallizing smallest-pore samples. The "internal" component (38, 39) is shown in Fig. 2B, where the data are compared with the results of the thermodynamic analysis of Fig. 2A. Although some alternatives to Oguni's analysis may be considered, the heat

nomenon, not a glass transition. The only irreversibility observed in Oguni *et al.*'s data was a very feeble "glass transition" (not visible on the scale of Fig. 2B) that occurred at 160 K. Confinement seems to act like a pressure (40) or, as shown in (41), like a change of potential such as to displace a liquid-liquid critical point from negative to positive pressures, which then has the same effect. This implies that bulk water behavior at ambient pressure would be either sharper than Fig. 2B, like the second of the Fig. 2A curves, or weakly first-order, as discussed below.

In light of Fig. 2, the atypically small value of the C_p "jump" at T_g of HQG and other low-density forms of amorphous water can be readily understood. At 136 K, Fig. 2B shows that there is almost nothing of the liquid-phase excess heat capacity left to lose at a glass transition. Thus, although the glass transition arrests the structure, most of the change in heat capacity, and creation of disorder upon heating, occurs in the subpeak part of the 225 K transition. This transition converts water continuously from a "fragile" molecular liquid above the transition to a "strong" liquid below it, so that water is a "strong" liquid as it vitrifies, as claimed in (13, 14). This picture suggests behavior akin to classical network glasses, which lie at the "strong" extreme of glass-formers and are also characterized by small heat capacity signatures at T_g and Arrhenius temperature dependences of transport coefficients above it [see also (42)].

The form of the excess C_p of water seen in Fig. 2 is completely different from that of common glass-formers but resembles that of the classical order-disorder transition seen in superlattice alloys and rotator phases. In this respect, it is compatible with the much-discussed "second critical point" interpretation of water's anomalies (43–45) because a critical point, associated with the vanishing of the transition order parameter, is the most interesting outcome of these cooperative excitation (order-disorder) processes. However, it is not the necessary, nor the most common, outcome, as considered further below.

Order-disorder transitions were at the center of interest in condensed matter physics half a century ago, but they are not often discussed in the current literature. Nonetheless, water (at least at low pressures) can be understood in terms of such a transition, as discussed below. However, it is useful to first consider a structural study by Mayer and co-workers (46) that suggests a rather abrupt crossover in the behavior of water during hyperquenching, which occurs in the vicinity of the heat capacity peak temperature of Fig. 2.

Mayer and co-workers used infrared spectroscopy to study the ion-pairing equilibrium in

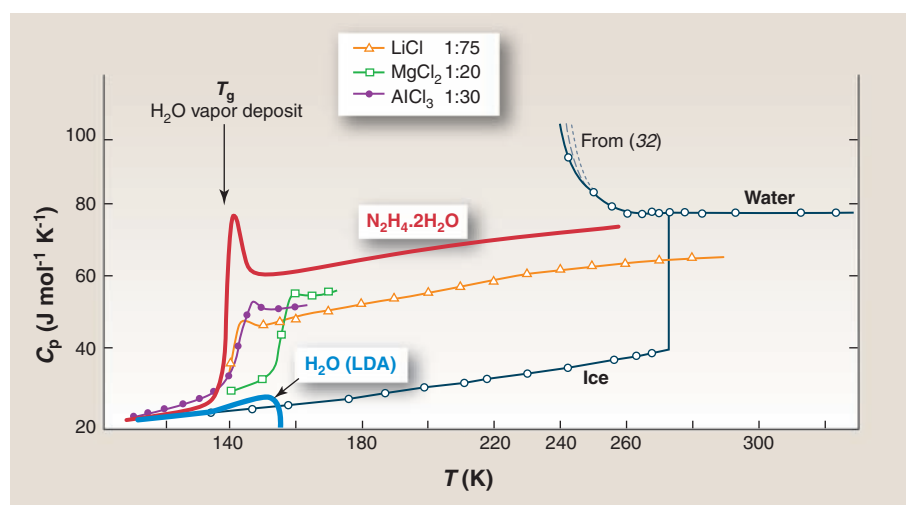


Fig. 1. Heat capacity data on water in supercooled and glassy forms, together with the heat capacities of molecular and ionic solutions in which the majority component is water. In the case of ionic solutions, the heat capacity reported is per mole of water. The plot for LDA is based on (29) (which established an LDA glass heat capacity of $2 \text{ J mol}^{-1} \text{ K}^{-1}$ above ice) and on (20) and (96) (which established the change of slope at 136 K, and crystallization temperature at $\sim 150 \text{ K}$, of annealed hyperquenched water). The curve for supercooled water combines the bulk water values to -30°C (35) with emulsion values to -38°C (32).

in which water does form the network but does not crystallize. The question is meaningful because we know that the glass can be produced from the ambient-pressure liquid by fast cooling (25, 36). Furthermore, liquid water can itself be generated (as tiny growing droplets from the supersaturated vapor) in this "gap" temperature range (37), and, in due course, it will be structurally characterized there as it is produced.

capacity revealed is remarkably similar to that given by the thermodynamic analysis at its more "smeared-out" limit, as shown in Fig. 2. When the heat capacity of ice is added to the thermodynamically deduced "excess heat capacity" of Fig. 2A, the agreement is almost quantitative. The striking feature of each curve is, of course, the peak at about 225 K. Note that this behavior is reversible; it is a liquid-state phe-

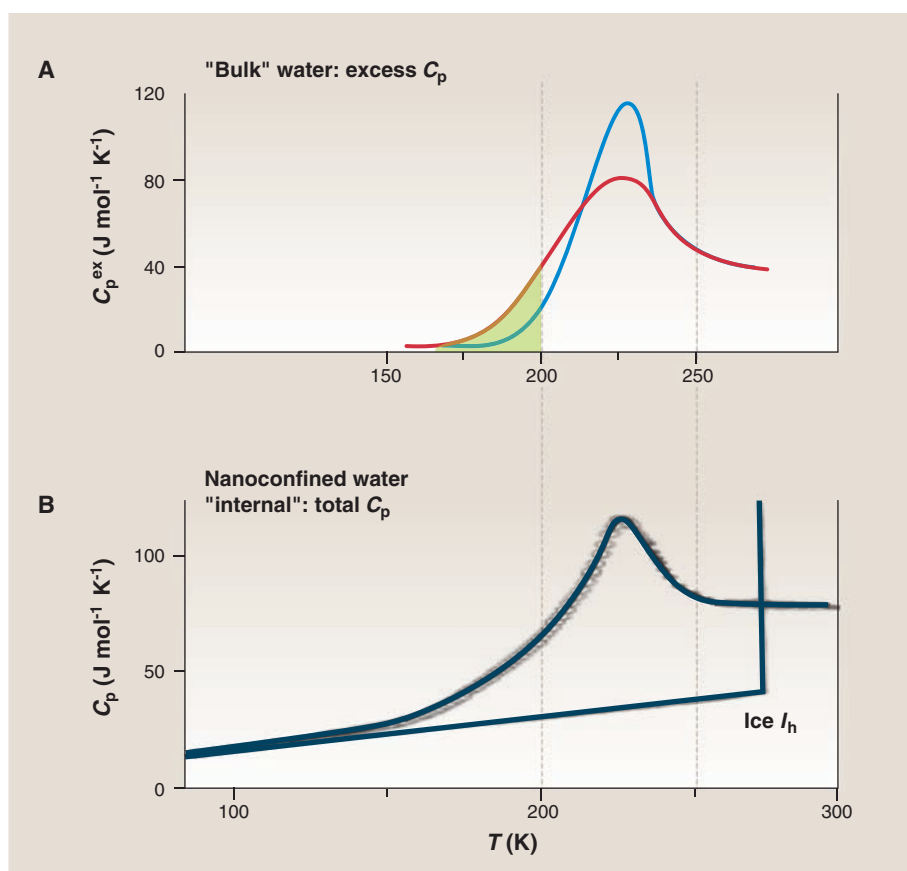


Fig. 2. (A) The molar excess heat capacity of supercooled water deduced by assuming phase continuity of supercooled water and vitreous ice and requiring adherence of water's properties to the first and second laws of thermodynamics through "no-man's land." The two curves delimit the range of possible C_p variations between 150 and 236 K allowed by the experimental data uncertainties. The shaded area is equivalent to 0.35 kJ. [From (15) by permission of Elsevier] (B) The total heat capacity of nanoconfined water, "internal" component, according to the measurements of Maruyama *et al.* [original data, as plotted in (38, 39)]. The peak temperature agrees well with the thermodynamic curve of upper panel for the more spread-out limit. Also, the heat capacity at the peak is near to the sum of this excess C_p in (A) and the heat capacity of ice at 225 K. Note the absence of any normal glass transition between 100 and 200 K (as in Fig. 1) visible on the scale of this figure. Small hysteretic anomalies are in fact detectable on more sensitive scales at 160 and 120 K [see (38, 39)]. [Reproduced by permission of Institute of Physics]

dilute solution between Ca^{2+} cations and NO_3^- anions in relation to temperature in the accessible temperature regime. By observing the ion pair distribution in the glass, they could tell, from the established temperature dependence, the "fictive" temperature T_f at which the equilibrium became "frozen in" during the hyperquench. The T_f they determined was high, between 200 and 230 K, hugely different from T_g determined in any other experiment. However, we can support their conclusion with thermodynamic data (also from Mayer's lab), along with Starr *et al.*'s thermodynamic analysis of Fig. 2A (15), as follows.

The immediate thermal rescan of a hyperquenched glass releases the frozen-in enthalpy in excess of that in the normal cooling glass transition, and is seen as a broad exothermic peak lying below T_g [see (24)]. This peak has been measured in several studies and has been used to determine T_f (47). In propylene glycol, quenched at the same rate as is used to vitrify water, T_f lies

25 K above the normal T_g (i.e., at 190 K). To show this for water, the shaded area under the broader curve of Fig. 2A is the frozen-in enthalpy of the Hallbrucker-Mayer HQG (48). Measured during rescan, as shown by the cross-hatched area in figure 1 of (49), it amounts to 0.19 kJ/mol (1/30th of the heat of crystallization) plus an extra 0.16 kJ/mol needed to allow for the (unusual) way the enthalpy recovery is cut short by the recrystallization in the case of HQG (48)—in all, 0.35 kJ/mol.

The upper bound of the shaded area in Fig. 2A should give an independent measure of T_f for the Mayer-Hallbrucker HQG. The result is seen in Fig. 2 is $T_f = 200$ K, which falls at the lower end (within the broad uncertainty range) of the ion pair probe method (46). At this temperature, we calculate [using the activation energy for diffusion in glassy water, 45 kJ/mol, reported by Kay at recent meetings (16), and assuming a preexponential constant of 10^{-14} s] that the relaxation time should

be about 10^{-4} s—which accords with the finding for hyperquenched propylene glycol (50).

In summary, there is evidence for a sudden change at around 200 K in the ability of water to equilibrate during hyperquenching. This value lies below the temperature of the C_p peak and presumably is the glass transition displaced to very high temperatures, in accord with Eq. 1, by the combination of high quenching rate and the Arrhenius ("strong liquid") character of the relaxation time in water below its C_p peak. This is fully consistent with the finding (51) that, during ultrafast heating, no glass transition is seen below 205 ± 5 K where crystallization occurs.

Order-Disorder Transitions

The above discussion builds a self-consistent picture, but I now argue that the understanding of water, given the limits on the direct measurements we can make, depends on our ability to integrate this tentative picture with the behavior of related systems and processes that are better understood—in this case, past studies of order-disorder processes (where the term is used in its older, general, pre-universality class, sense, as we are not concerned with behavior near the peak). Of special relevance are those cases that have been shown to have ergodicity-breaking "transitions" in their tail ends.

The most directly comparable case we find is that of the rotator phase of the fullerene C_{60} , which is dielectrically active in its crystalline state. This system has been studied by many workers using different techniques, particularly dielectric relaxation (52), heat capacity (53), and the related enthalpy relaxation process (53). Some data are reproduced in Fig. 3. The total heat capacity exhibits a sharp peak at 250 K—the rotator phase transition (Fig. 3A). The relaxation time for re-orientation of the polar defects has been measured by dielectric relaxation (52) and is perfectly Arrhenius in character between 100 K and the phase transition at 250 K (11 orders of magnitude in τ). It blends smoothly with the longer relaxation times measured by enthalpy relaxation, which are shown in the Arrhenius plot of Fig. 3C. The value at 90 K is 1000 s and is characteristic of the glass transition when measured at the slow effective scan rate of adiabatic calorimetry, 0.1 K/min. In differential scanning calorimetry (DSC) at 10 K/min, it would be observed where $\tau_{HI} = 100$ s (i.e., at 91.3 K). This experiment identifies unambiguously the tiny step at 90 K as the ergodicity-restoring glass transition for this system, which is shown on an expanded scale in Fig. 3B. It is thus a "glassy crystal" but one that terminates its configurational excitation in a continuous order-disorder transition (λ transition) rather than in a first-order melting transition, as in the usual case. This happens because fullerenes cannot melt even at high pressures, in consequence of their critical temperatures falling within their solid-phase stability domains (54). They can only sublime.

We see that the magnitude of the glass transition in C_{60} is even smaller than that for water. Being so weak, it would not be detected using ordinary DSC

procedures. The phase transition temperature, 250 K, lies somewhat above that for water. The greater disordering range, 91 to 250 K, is consistent with the smaller activation energy for excitation [28.6 kJ/mol (52) versus 45 kJ for water (16)].

Although no “hyperquench and scan” studies have been made on the very weak “glass transition” seen in the tail of the C_{60} disordering transition (53) (Fig. 3B), it is reasonable to expect to see, in such studies, the same phenomena exhibited by water (48). Indeed, this should be seen in any of the familiar λ transitions (NaNO_3 , etc.) when examined with sufficient precision. More important, they may also be seen in cases such as KNO_3 in which the λ transition is interrupted by a first-order transition to the higher-temperature, more disordered, phase. According to current practice, all should be termed “glass transitions” because in each case a residual disorder is frozen in below the “glass temperature.” That the disordering occurs within a crystal, not a glass, is not of concern here. Premelting phenomena in many crystals fall into the same class, and their fast quenching and reheating behavior should likewise be examined for “glass transitions” associated with the freezing-in of crystalline disorder. All will be very weak, like that of water. The effect of the freezing-in of defect concentration on the ionic conductivity of crystals is known; it resembles the effect of the glass transition on the conductivity of ion-conducting glasses (55). Both resemble the “fragile-to-strong” transition currently much discussed in confined water (56), but are in fact quite different because they depend entirely on ergodicity-breaking at the transition.

Which type of glass transition is the more “interesting” is a matter of taste, but it is clear that those occurring in the tails of λ transitions are glass transitions that are stripped of the mystery and the challenge of the glass transition that current theory strives to resolve (8, 57–66). There is no Kauzmann paradox demanding resolution, and no hidden first- or second-order transitions to be discussed and contested. As a class, λ transitions have been intensively studied, and their heat capacity forms are quite well understood. It is interesting to

note, however, that two of the current group of theoretical approaches to the glass transition (59, 67) obtain considerable success in describing the supercooled liquid heat capacity behavior with excitation thermodynamics mathematically equivalent to that of the popular, although approximate, Bragg-Williams theory for the order-disorder transition, originally invented to describe disordering in alloys such as AuCu (1:1). This is

also the property of the Moynihan model of polyamorphism in water (68) discussed below.

The Energy Landscape

What distinguishes a λ transition with ergodicity breaking (i.e., glass transition) in its tail, as in Fig. 3, from a “normal” glass transition? Operationally, it is that in the former, the peak in the configurational heat capacity lies in the ergodic domain, whereas in the latter, it is hidden below the glass transition. Kinetically, it reflects the ease with which the system can explore its potential energy hypersurface without getting “stuck.” Thus, the potential energy landscape (PEL) for water must have very shallow “basins of attraction” (69) so that it can deexcite with temperature decrease, even at low temperatures. On accessible time scales, it can then approach closely the global minimum on its PEL. The glass transition interrupts only the final approach to the global minimum, so that the “ideal” glass state becomes (almost) accessible in the same way (70) as the “folding funnel” (71) makes the global minimum accessible to protein molecules. The entropy for water near its T_g is indeed remarkable for its small value (72, 73), rivaled only by vitreous BeF_2 (42).

Although the ergodicity-breaking phenomenon in water may therefore be simpler to interpret than that in normal glass-formers, it is by no means less important. Indeed, it allows us to shine light on broader aspects of viscous liquid thermodynamics and on the whole strong/fragile liquid phenomenology of glass-formers, as described in (42).

The Fragile-to-Strong Crossover in Supercooled Water

Let us consider how all the foregoing can help us understand another striking feature of the behavior of liquid water, the fragile-to-strong transition, that is observed indirectly upon hyperquenching. Long only an inferred phenomenon (13–15), this abrupt change in the temperature dependence of relaxation processes in supercooling water (15) has now been directly observed, for both diffusivity and relaxation time, by Chen and colleagues (56, 74, 75). They achieved this by study of water samples sequestered in nanoscopic (1.5 nm diameter) tubule arrays, in which the water does not crystallize. The most extensive data come from the pulsed field gradient spin-echo diffusivity study of Mallamace *et al.* (56) in which the break in temperature dependence of the diffusivity occurs at 220 K—the same temperature seen in Fig. 2 for the peak in the nanosample heat capacity (38, 39). Although the nano-sequestration clearly changes the behavior of the water (40, 41, 76), it is to damp out, rather than to exaggerate, the behavior in real water. These changes are attributed to a Widom (supercritical fluctuations) line crossing by Stanley and co-workers (77) (see below). Alternatively, some authors attribute them to confinement length scale effects (78). In any case, a strong-fragile transition is a direct prediction of Fig. 2 via the Adam-Gibbs equation (79), $\tau = \tau_0 \exp(C/TS_c)$, where S_c is the configurational entropy and τ_0 and C are

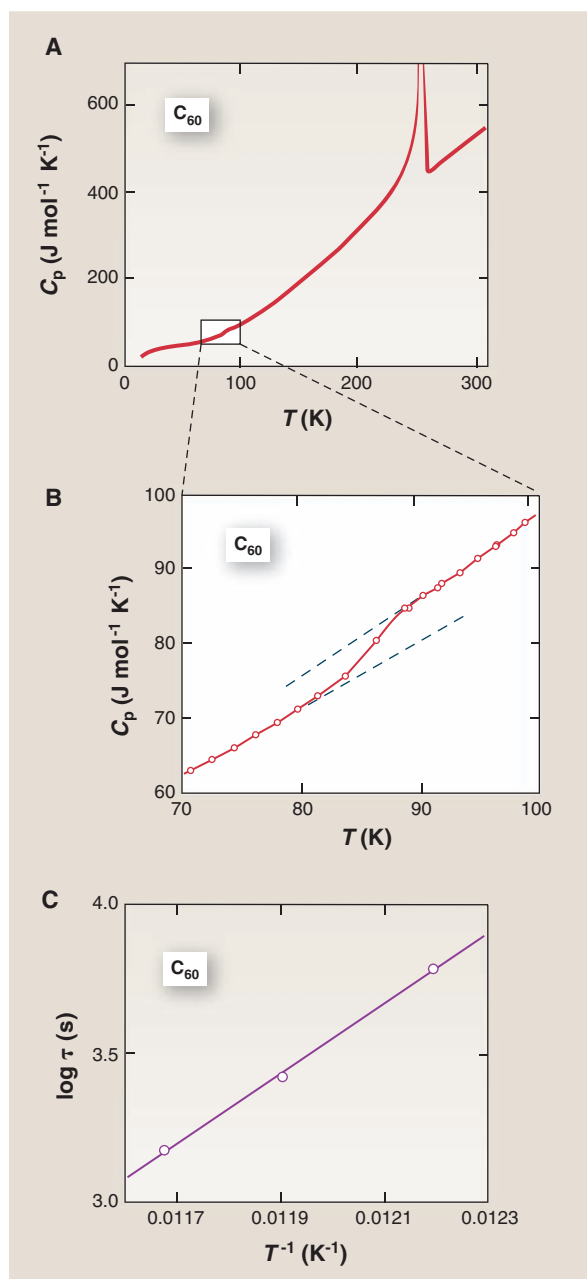


Fig. 3. The λ transition and glass transition for the rotator phase of C_{60} . (A) The full transition, showing the peak of the transition (where the order parameter vanishes) at 250 K. The box at the lower left is enlarged in (B) to show the heat capacity anomaly (glass transition) at 83 to 88 K. (C) Arrhenius plot of the enthalpy relaxation time for C_{60} , from which the relaxation time at the onset of the glass transition is seen to be 104 s. In a “standard” DSC scan, the onset would be at 91.3 K, which can be predicted from Eq. 1 using the activation energy measured in (52). [From (53) by permission]

constants. This relation requires the temperature dependence of any relaxation process to change sharply when the heat capacity peaks, as demonstrated in figure 3 of (15).

Order-Disorder Versus "Second Critical Point" Scenarios

As already stated, the present interpretation invoking order-disorder phenomenology is compatible with a critical point interpretation of supercooled water phenomenology. However, it does not require that a critical point exist. The majority of order-disorder processes end in first-order phase transitions to the disordered state. For bulk water at ambient pressure and excluding crystallization, it remains possible that the thermal excitation of the low-density liquid (LDL) phase [or the supercooling of the high-density liquid (HDL) phase] may terminate in first-order phase transitions. Indeed, a first-order phase transition is what is implied by the power-law fits of data in much of the supercooled water (HDL) literature (1, 2, 35, 80, 81) [and also what is found (67) in an excitations model best fit to the low-temperature LDL (confined water) heat capacity data in Fig. 2]. It is also what is required by the phase diagram derived (82) from the Haar-Gallagher-Kerr equation of state, which was long considered the best description of water in its stable state, and which has proven capable of predicting the behavior of water in the homogeneous nucleation (kinetic) limit of its metastable stretched state (83). This phase diagram predicts distinct and different tensile limits for HDL and LDL.

Power laws imply diverging fluctuations. They arise by approach either to a critical point or to one of the spinodal lines that radiate out from a critical point. In the latter case, a first-order transition must be crossed before the critical divergence temperature is reached, as seen in the case of the water analog, liquid silicon, in (84).

The properties that have been measured to the lowest temperature in ambient-pressure supercooled water are the spin-lattice relaxation time T_1 and the viscosity. T_1 can be studied in the presence of crystalline ice (e.g., in emulsion samples) without loss of precision because the crystal signal is not motionally narrowed. In (2), data down to 238 K were fit by a power law with the same singular temperature, 228 K (233 K for D_2O), that had earlier been obtained from fits to data on other properties (5, 85, 86). Note that there is only a narrow range, 10 K, in which to encounter either a major deviation from the power law or, alternatively, the intervening liquid-liquid phase transition. Only the T_1 plots for protons (or deuterons) show any deviations from the power law, and protons (deuterons) are known to decouple from oxygen motions by the Grotthuss mechanism. It is plausible that the sharp, seemingly inevitable, crystallization that occurs at 234 K in these slowly cooled samples is the result of encountering the phase transition to the fast-crystallizing LDL phase, because this would revisit what has already been seen repeatedly (84, 87)

in liquid silicon, and indeed in TIP4P water (Ewald summation version) in simulation (88).

What is different here from the original Speedy-Angell proposition (85, 86) is the recognition that the spinodal, rather than existing alone as the unique endpoint of the liquid state, in fact underlies a phase transition to the new liquid phase, LDL, as indeed the phase diagram of (82) would imply. Interestingly enough, the first-order transition temperature obtained in (67) from the fit of an order-disorder excitations theory to the confined water LDL C_p data seen in Fig. 2 falls at 229 K (67)—slightly above the HDL spinodal, as it should. Furthermore, this must be a minimum value because it is based on fitting data for water in hydrophilic confinement, for which the critical point is [according to simulations (41)] pushed from negative to positive pressures. According to the phase diagram of (82), this first-order liquid-liquid transition description actually belongs to a "critical point-free" scenario, which is quite distinct from both "second critical point" (3, 31, 43) and "singularity-free" (3, 31, 89) alternatives. In this respect it lies at the opposite extreme from the "singularity-free" scenario (89), which requires T_c to retreat to 0 K (3). The critical point-free scenario, or a variant in which the second critical point exists but only at negative pressure, are supported by the observation that all ambient-temperature response functions and transport coefficients appear to be diverging at the same singular temperature (2, 80, 81, 85, 86), a behavior not found much beyond the critical point (77).

Countering the critical point-free scenario are two cooperative excitation models, the Moynihan two species-nonideal solution model (68) and the Franzese-Marques-Stanley intramolecular coupling model (90, 91), each of which yields a liquid-liquid critical point at positive pressure. In this case the fragile-strong transition becomes, at ambient pressure, a continuous transition associated with crossing the "Widom line" (the higher-order extension of the coexistence line beyond the critical point). The Moynihan model in particular inputs data from the experimental hysteresis of the LDA-HDA polyamorphic transition (27) as spinodal pressure limits, and derives a critical pressure of 380 atm. This is remarkably close to the value of 270 atm deduced by Fuentavilla and Anisimov (92) from critical scaling law fitting of the bulk water heat capacity and compressibility data. The latter analysis gave a critical temperature of 232 K, which is unfeasibly high, whereas the Moynihan model gives 225 K. However, the absence of any sign of power-law breakdown for the ambient-pressure properties, except for those known to decouple, is a problem for these models. The ^{17}O T_1 measurements in coldest emulsions (93) bear repeating with modern equipment because they appear to be crucial in determining the most plausible description of this important liquid.

Concluding Remarks

There is not much distinction between the order-disorder transition scenario we have

outlined here and the second critical point scenario, which associates all water anomalies with the existence of a second critical point. Is the second critical point to be regarded as the source of the anomalies of water, or is the cooperativity of the configurational excitations (implied by the form of the heat capacity that we have extracted) to be seen as the primary phenomenon to be interpreted—one that may, at some parameter or some thermodynamic field choice, produce a critical point? It becomes a "chicken or egg" issue, and the question is: Which is scientifically the more fruitful? When a critical point exists, all of the universalities that are implied (near the transition) can be enjoyed, but if the cooperativity is insufficient to induce a critical point, the liquid can still have interesting and important practical properties, such as a vanishing expansion coefficient (as in SiO_2). Indeed, the relation of water to SiO_2 glass and liquid, and the "big picture" of glass-formers, is a vitally interesting question—which is taken up elsewhere (42).

References and Notes

1. E. W. Lang, H. D. Lüdemann, *Angew. Chem. Int. Ed. Engl.* **21**, 315 (1982).
2. C. A. Angell, *Annu. Rev. Phys. Chem.* **34**, 593 (1983).
3. P. G. Debenedetti, *J. Phys. Condens. Matter* **15**, R1669 (2003).
4. A "phase transition" is a "singularity," an event that totally separates the substance on one side of the transition from the substance on the other side. For a pure substance, this happens in a reversible manner. For instance, in the case of melting at constant pressure, once the pressure is fixed there is only one temperature at which the two phases, liquid and crystal, can coexist. At any other temperature, it is one or the other of the two—an "all-or-nothing" situation.
5. M. Oguni, C. A. Angell, *J. Chem. Phys.* **73**, 1948 (1980).
6. We like to define T_g as the onset value obtained when scanning at 20 K/min, after cooling at a standard rate of 20 K/min, because at that temperature the relaxation time is close to 100 s and therefore agrees with the value reported by relaxation spectroscopists, who define T_g as the temperature at which the relaxation time is 100 s (94).
7. F. Stickel, E. W. Fischer, R. Richert, *J. Chem. Phys.* **102**, 6251 (1995).
8. J. Dyre, *Rev. Mod. Phys.* **78**, 953 (2006).
9. C. A. Angell, *J. Therm. Anal. Calorim.* **69**, 785 (2002).
10. C. A. Angell, *Science* **267**, 1924 (1995).
11. N. Giovambattista, C. A. Angell, F. Sciortino, H. E. Stanley, *Phys. Rev. Lett.* **93**, 047801 (2004).
12. A. Minoguchi, R. Richert, C. A. Angell, *Phys. Rev. Lett.* **93**, 215703 (2004).
13. C. A. Angell, *J. Phys. Chem.* **97**, 6339 (1993).
14. K. Ito, C. T. Moynihan, C. A. Angell, *Nature* **398**, 492 (1999).
15. F. Starr, C. A. Angell, H. E. Stanley, *Physica A* **323**, 51 (2003).
16. B. D. Kay *et al.*, Abstracts of papers of the American Chemical Society 229: U706-U706 024-PHYS Part 2 (2005).
17. S. M. McClure, D. J. Safarik, T. M. Truskett, C. B. Mullins, *J. Phys. Chem. B* **110**, 11033 (2006).
18. D. Kivelson, G. Tarjus, *J. Phys. Chem. B* **105**, 6220 (2001).
19. R. S. Smith, B. D. Kay, *Nature* **398**, 788 (1999).
20. I. Kohl, L. Bachmann, E. Mayer, A. Hallbrucker, T. Loerling, *Nature* **435**, E1 (2005).
21. The most recent assessment of the laboratory glass transition in water (20) reports $\Delta C_p = 0.7 \text{ J K}^{-1} \text{ mol}^{-1}$ compared with $35 \text{ J K}^{-1} \text{ mol}^{-1}$ for $(H_2O)_2 \cdot H_2O_2$.
22. J. A. Pryde, G. O. Jones, *Nature* **170**, 685 (1952).
23. D. R. MacFarlane, C. A. Angell, *J. Phys. Chem.* **88**, 759 (1984).
24. Y. Z. Yue, C. A. Angell, *Nature* **427**, 717 (2004).
25. E. Mayer, *J. Appl. Phys.* **58**, 663 (1985).
26. E. F. Burton, W. F. N. Oliver, *Nature* **135**, 505 (1935).

27. O. Mishima, *J. Chem. Phys.* **100**, 5910 (1994).
28. A highly analogous behavior has recently been observed for the element germanium, which shares with water an open tetrahedral crystal ground state and an increase in density upon fusion. It can be obtained in the amorphous form by different methods, vapor deposition, electrodeposition, and quenching of flame-formed droplets, and these forms are apparently identical. It has recently been shown (95) that a dense glassy form, obtained by quenching the high-pressure metallic liquid, undergoes a polymorphic phase change, during pressure decrease at ambient temperature, to yield a glass that is essentially the same as that formed at low pressure, although with small displacements in the structure factor $S(q)$ peak positions.
29. Y. P. Handa, D. D. Klug, *J. Phys. Chem.* **92**, 3323 (1988).
30. A. Hallbrucker, E. Meyer, G. P. Johari, *J. Phys. Chem.* **93**, 4986 (1989).
31. H. E. Stanley, P. G. Debenedetti, *Phys. Today* (2005).
32. C. A. Angell, W. J. Sichina, M. Oguni, *J. Phys. Chem.* **86**, 998 (1982).
33. D. H. Rasmussen, A. P. Mackenzie, J. C. Tucker, C. A. Angell, *Science* **181**, 4079 (1973).
34. G. P. Johari, *J. Chem. Phys.* **107**, 10154 (1997).
35. E. Tombari, C. Ferrari, G. Salvetti, *Chem. Phys. Lett.* **300**, 749 (1999).
36. O. Mishima, *J. Chem. Phys.* **121**, 3161 (2004).
37. Y. J. Kim, B. E. Wyslouzil, G. Wilemski, J. Wölk, R. Strey, *J. Phys. Chem. A* **108**, 4365 (2004).
38. S. Maruyama, K. Wakabayashi, M. A. Oguni, *AIP Conf. Proc.* **708**, 675 (2004).
39. M. Oguni, S. Maruyama, K. Wakabayashi, A. Nagoe, *Chem. Asian J.* **2**, 514 (2007).
40. C. A. Angell, *Nature Nanotechnol.* **2**, 396 (2007).
41. I. Brovchenko, A. Oleinikova, *J. Chem. Phys.* **126**, AN214701 (2007).
42. C. A. Angell, *Bull. Mater. Res. Soc.* (Turnbull lecture) (February 2007); arxiv.org/abs/0712.4233.
43. P. H. Poole, F. Sciortino, U. Essmann, H. E. Stanley, *Nature* **360**, 324 (1992).
44. F. Sciortino, P. H. Poole, U. Essmann, H. E. Stanley, *Phys. Rev. E* **55**, 727 (1997).
45. H. E. Stanley *et al.*, *Physica A* **236**, 19 (1997).
46. G. Fleissner, A. Hallbrucker, E. Meyer, *J. Phys. Chem. B* **102**, 6239 (1998).
47. L.-M. Wang, C. A. Angell, *J. Non-Cryst. Solids* **353**, 3829 (2007).
48. A. Hallbrucker, E. Meyer, G. P. Johari, *J. Phys. Chem.* **93**, 4986 (1989).
49. V. Velikov, S. Borick, C. A. Angell, *Science* **294**, 2335 (2001).
50. C. A. Angell *et al.*, *J. Phys. Condens. Matter* **15**, S1051 (2003).
51. M. Chonde, M. Brindza, V. Sadtchenko, *J. Chem. Phys.* **125**, 094501 (2006).
52. P. Mondal, P. Lunkenheimer, A. Loidl, *Z. Phys. B* **99**, 527 (1996).
53. T. Matsuo *et al.*, *Solid State Commun.* **83**, 711 (1992).
54. M. H. J. Hagen, E. J. Meijer, G. C. A. M. Moolj, *Nature* **365**, 425 (1993).
55. F. Mizuno *et al.*, *J. Non-Cryst. Solids* **352**, 5147 (2006).
56. F. Mallamace *et al.*, *J. Chem. Phys.* **124**, 161102 (2006).
57. H. Tanaka, *J. Phys. Cond. Matter* **111**, 3175 (1999).
58. H. Tanaka, *Phys. Rev. E* **62**, 6978 (2000).
59. C. A. Angell, C. T. Moynihan, *Metall. Mater. Trans. B* **31**, 587 (2000).
60. X. Xia, P. G. Wolynes, *Proc. Natl. Acad. Sci. U.S.A.* **97**, 2990 (2000).
61. D. V. Matyushov, C. A. Angell, *J. Chem. Phys.* **123**, 034506 (2005).
62. H. Tanaka, *Phys. Rev. Lett.* **90**, 055701 (2003).
63. J. P. Garrahan, D. Chandler, *Proc. Natl. Acad. Sci. U.S.A.* **100**, 9710 (2003).
64. G. Biroli, J.-P. Bouchaud, G. Tarjus, *J. Chem. Phys.* **123**, 044510 (2005).
65. D. Chandler, J. P. Garrahan, *J. Chem. Phys.* **123**, 044511 (2005).
66. P. G. Debenedetti, F. H. Stillinger, M. S. Shell, *J. Phys. Chem. B* **107**, 14434 (2003).
67. D. V. Matyushov, C. A. Angell, *J. Chem. Phys.* **126**, 094501 (2007).
68. C. T. Moynihan, *Proc. Mat. Res. Soc. Symp.* **455**, 411 (1997).
69. F. H. Stillinger, *Science* **267**, 1935 (1995).
70. C. A. Angell, *Philos. Trans. R. Soc. London Ser. A* **363**, 415 (2005).
71. P. G. Wolynes, J. N. Onuchic, D. Thirumalai, *Science* **268**, 960 (1995).
72. R. J. Speedy, P. G. Debenedetti, R. S. Smith, C. Huang, B. D. Kay, *J. Chem. Phys.* **105**, 240 (1996).
73. E. Whalley, D. D. Klug, Y. P. Handa, *Nature* **342**, 782 (1989).
74. A. Faraone, L. Liu, C. Y. Mou, C. W. Yen, S. H. Chen, *J. Chem. Phys.* **121**, 10843 (2004).
75. L. Liu, A. Faraone, C. Mou, C. W. Yen, S. H. Chen, *J. Phys. Condens. Matter* **16**, S5403 (2004).
76. J. Rault, R. Neflati, P. Judenstein, *Eur. Phys. J. B* **36**, 627 (2003).
77. L.-M. Xu *et al.*, *Proc. Natl. Acad. Sci. U.S.A.* **102**, 16558 (2005).
78. J. Swenson, H. Jansson, R. Bergman, *Phys. Rev. Lett.* **96**, 247802 (2006).
79. G. Adam, J. H. Gibbs, *J. Chem. Phys.* **43**, 139 (1965).
80. B. D. Cornish, R. J. Speedy, *J. Phys. Chem.* **88**, 1888 (1984).
81. W. S. Price, H. Ide, Y. Arata, *J. Phys. Chem. A* **103**, 448 (1999).
82. Q. Zheng *et al.*, in *Liquids Under Negative Pressures*, A. R. Imre, H. J. Maris, P. R. Williams, Eds. (Kluwer Academic, Dordrecht, Netherlands, 2002), pp. 33–46.
83. Q. Zheng, D. J. Durben, G. H. Wolf, C. A. Angell, *Science* **254**, 829 (1991).
84. S. Sastry, C. A. Angell, *Nat. Mater.* **2**, 739 (2003).
85. R. J. Speedy, C. A. Angell, *J. Chem. Phys.* **65**, 851 (1976).
86. R. J. Speedy, *J. Phys. Chem.* **86**, 982 (1982).
87. C. A. Angell, S. Borick, M. Grabow, *J. Non-Cryst. Solids* **205–207**, 463 (1996).
88. M. Matsumoto, A. Saito, I. Ohmine, *Nature* **416**, 409 (2002).
89. S. Sastry, P. G. Debenedetti, F. Sciortino, H. E. Stanley, *Phys. Rev. E* **53**, 6144 (1996).
90. G. Franzese, M. I. Marques, H. E. Stanley, *Phys. Rev. E* **67**, 011103 (2003).
91. G. Franzese, H. E. Stanley, *J. Phys. Cond. Matter* **19**, 205126 (2007).
92. D. A. Fuentevilla, M. A. Anisimov, *Phys. Rev. Lett.* **97**, 195702 (2006).
93. J. C. Hindman, *J. Chem. Phys.* **60**, 4488 (1974).
94. C. A. Angell, *Chem. Rev.* **102**, 2627 (2002).
95. H. Bhat *et al.*, *Nature* **448**, 787 (2007).
96. K. Hofer, E. Meyer, G. P. Johari, *J. Phys. Chem.* **95**, 7100 (1991).
97. Supported by the NSF under Solid State Sciences grant DMR 0454672 and Chemical Sciences grant 0404714.

I thank V. Molinero and P. G. Debenedetti for important critical comments on earlier versions of this manuscript, and H. E. Stanley, S. Buldyrev, F. Sciortino, C. T. Moynihan, and D. V. Matyushov for helpful discussions.

10.1126/science.1131939